THE JOURNAL OF BIOLOGICAL CHEMISTRY VOL. 287, NO. 17, pp. 13899–13910, April 20, 2012

Combined Analysis of MicroRNome and 3′-UTRome Reveals a Species-specific Regulation of Progesterone Receptor Expression in the Endometrium of Rhesus Monkey*[S]

Received for publication, September 6, 2011, and in revised form, February 12, 2012 Published, JBC Papers in Press, February 29, 2012, DOI 10.1074/jbc.M111.301275

Ji-Long Liu[‡1], Xiao-Huan Liang[‡1], Ren-Wei Su[§], Wei Lei[§], Bo Jia[¶], Xu-Hui Feng[¶], Zhi-Xiong Li[‖], and Zeng-Ming Yang[‡¶2]

From the [‡]Department of Biology, Shantou University, Shantou 515063, China, the [§]College of Life Science, Northeast Agricultural University, Harbin 150030, China, the [¶]School of Life Science, Xiamen University, Xiamen 361005, China, and the [‖]Fujian Non-Human Primate Research Center, Fujian Family Planning Institute, Fuzhou 350011, China

Background: The contribution of endometrial microRNAs (miRNAs) to female reproduction in rhesus monkey is unknown.
Results: Progesterone receptor is negatively modulated by miRNAs through non-conserved miRNA binding sites in the 3′-UTR.
Conclusion: miRNA regulation of endometrial receptivity is species-dependent.
Significance: Our study provides new insights into the species-biased molecular mechanisms underlying endometrial receptivity from the aspects of miRNA-mediated regulation.

The establishment of endometrial receptivity is a prerequisite for successful pregnancy, which is controlled by a complex mechanism. MicroRNAs (miRNAs) are small non-coding RNAs that have emerged as important regulators of gene expression. However, the contribution of miRNAs in endometrial receptivity is still unknown. Here we used rhesus monkey as an animal model and compared the endometrial miRNA expression profiles during early-secretory (pre-receptive) phase and mid-secretory (receptive) phase by deep sequencing. A set of differentially expressed miRNAs were identified, 8 of which were selected and validated using quantitative RT-PCR. To facilitate the prediction of their target genes, the 3′-UTRome was also determined using tag sequencing of mRNA 3′-termini. Surprisingly, about 50% of the 10,677 genes expressed in the rhesus monkey endometrium exhibited alternative 3′-UTRs. Of special interest, the progesterone receptor (*PGR*) gene, which is necessary for endometrial receptivity, processes an ultra long 3′-UTR (~10 kb) along with a short variant (~2.5 kb). Evolutionary analysis showed that the 3′-UTR sequences of *PGR* are poorly conserved between primates and rodents, suggesting a species-biased miRNA binding pattern. We further demonstrated that *PGR* is a valid target of *miR-96* in rhesus monkey and human but not in rodents, whereas the regulation of *PGR* by *miR-375* is rhesus monkey-specific. Additionally, we found that *miR-219–5p* regulates *PGR* expression through a primate-specific long non-coding RNA immediately downstream of the *PGR* locus. Our study provides new insights into the molecular mechanisms underlying endometrial receptivity and presents intriguing species-specific regulatory roles of miRNAs.

The establishment of endometrial receptivity to embryo implantation is a prerequisite for the success of human reproduction. Endometrial receptivity is strictly controlled by the ovarian steroid hormones, estrogen, and progesterone, through their nuclear receptors (1). Although both ovarian progesterone and estrogen are needed for embryo implantation in rats and mice (2), progesterone alone may be sufficient in some other species, such as rhesus monkeys and humans (3, 4). However, the molecular mechanism underlying progesterone regulation of endometrial receptivity is still poorly understood.

Recently, microRNAs (miRNAs)[3] have emerged as important regulators of gene expression. miRNAs are a class of ~22 nucleotides (nt) long non-coding RNAs processed from long primary transcripts via consecutive cleavage by two RNase III enzymes, Drosha and Dicer. Mature miRNAs recognize target mRNAs by imperfect base-pairing to complementary target sites, typically in the 3′-untranslated region (3′-UTR), leading to translational repression and/or mRNA degradation (5). In humans, more than 1,000 miRNAs have been discovered (miRBase Release 16). Since each miRNA is capable of targeting several hundred mRNAs, more than 60% of protein-coding genes are predicted to undergo direct miRNA regulation (6). Thus, miRNAs provide a widespread mechanism to control gene expression. Studies have indicated that miRNAs play an important role in the postnatal development of mouse uterus and oviduct (7–9). Uterine miRNAs are expressed in a steroid hormone-dependent manner in mice (10), and several groups have demonstrated that miRNA expression profiles change

* This work was supported by the National Basic Research Program of China (2011CB944402) and the National Natural Science Foundation of China (30930013 and 31071276).
[S] This article contains supplemental Tables S1–S3.
[1] Both authors contributed equally to this work.
[2] To whom correspondence should be addressed: Department of Biology, Shantou University, Shantou 515063, China. Tel.: 86-754-82902011; E-mail: zmyang@stu.edu.cn.

[3] The abbreviations used are: miRNA, microRNA; IVF, *in vitro* fertilization; 3′-UTR, 3′-untranslated region; PGR, progesterone receptor; lncRNA, long non-coding RNA.

dynamically in the uterus during embryo implantation in mice and humans (11–14).

In this study, we aimed to study the contribution of miRNAs in endometrial receptivity using the rhesus monkey as an animal model. Because of ethical restrictions and experimental difficulties, it is not practical for direct analysis of embryo implantation process in humans (15, 16). Current studies heavily rely on mice. Mice are easy to maintain and handle, and reproduce quickly. Most importantly, the mouse genome supports targeted mutagenesis in specific genes by homologous recombination in embryonic stem (ES) cells, which allows genes to be altered efficiently and precisely (16). However, a recent study has indicated that null mutations in human and mouse orthologs frequently result in different phenotypes, suggesting that results from mouse models should be extrapolated to humans with caution (17). In particular, there are considerable differences in morphological changes, hormonal dependence, and molecular interactions between mice and humans during embryo implantation (18). Therefore, non-human primates are ideal models for studying endometrial receptivity and embryo implantation in humans.

Rhesus monkeys (*Macaca mulatta*) are the most frequently used laboratory non-human primates. They have a regular menstrual cycle (~28 days), similar to women. However, the genomic resources for the rhesus monkey are relatively limited. The current list of rhesus monkey miRNAs reported in miRBase is still largely incomplete (comprising only 479 sequences, miRBase Release 16), most of which were identified by searching the rhesus monkey genome for human miRNA homologs (19). Given that microarray are restricted to detect known miRNA sequences and have some limitations in quantification due to nonspecific hybridization (20), we constructed two small RNA libraries from the endometrium samples collected on menstrual cycle days 15 (pre-receptive phase) and 21 (receptive phase) and subjected to direct deep sequencing. Deep sequencing measures the copy numbers of small RNA sequences, thus allowing for the discovery of novel miRNAs (20, 21). Additionally, most rhesus monkey genes have lacked annotated 3′-UTRs, making it hard to predict miRNA target genes. Although human 3′-UTRs can be used to predict homologous 3′-UTRs in the rhesus monkey, previous studies have indicated that alternative polyadenylation pattern of genes varies across tissues and developmental stages (22–24). Therefore, we also determined the 3′-UTRome using 3′-end tag sequencing of mRNA termini. Joint analysis of microRNome and 3′-UTRome enables us to characterize the role of miRNAs in endometrial receptivity. Through data mining followed by experimental validation, we found that the progesterone receptor gene (*PGR*) is negatively regulated by several miRNAs that are highly expressed in receptive endometrium in a species-specific manner. Our approach represents a novel strategy for regulatory and functional studies on miRNAs.

EXPERIMENTAL PROCEDURES

Tissue Collection—Healthy and mature female rhesus monkeys (*Macaca mulatta*) were housed singly in a controlled environment with a 12 h light/12 h dark cycle at the Fuzhou Nonhuman Primate Research Center (Fujian, China). All female rhesus monkeys were evaluated daily by visual examination of the perineum for menses, with the onset of menses defined as day 1 of the menstrual cycle. Female rhesus monkeys showing at least two consecutive menstrual cycles of ~28 days were chosen for this study. Serum estrogen concentration was measured daily to screen estrogen peak. Both estrogen peak and the dating of menstrual cycle were used to determine the time of ovulation (25). Endometrial tissues were collected on day 15 (pre-receptive phase, $n = 3$) and day 21 (receptive phase, $n = 3$) of menstrual cycle by hysterectomy. Samples were flash-frozen in liquid nitrogen and stored at −80 °C for further analysis. This study design was approved by the Institutional Animal Care and Use Committee of Shantou University.

Deep Sequencing of miRNAs—Total RNAs of rhesus monkey endometrial tissues were extracted using TRIzol reagent (Invitrogen). Small RNAs in the size range of 18~30 nt were purified from denaturing 15% polyacrylamide gel and ligated with adapters. After purification, small RNAs were reverse transcribed and amplified for 15 cycles. PCR products were purified and quantified for high-throughput sequencing with the Illumina Genome Analyzer IIx at Huada Genomics Institute Co. Ltd (Shenzhen, China).

A computational pipeline was used to process the sequencing data. All small RNA reads without perfect matches to the most proximal 8 nt of the 5′-adaptor sequences were removed. The adaptor-free reads were then queried against known miRNA and other non-coding RNAs obtained from miRbase release 16, piRNABank version 2.0 and fRNAdb version 3.4 using the Bowtie align tool version 0.9.9.1 (51). The miRNA expression profile was calculated by summing the number of reads that mapped uniquely to known miRNAs. Read counts were then normalized to reads per million in each dataset, and fold changes between datasets were calculated according to normalized read counts. When comparing two groups of profile differences, a two-sided z-test with Bonferroni multiple test correction was employed. The fold change values in miRNA expression between groups were also calculated. Differentially expressed miRNAs were chosen according to the criteria of a fold-change greater than 2 and a p value less than 0.001.

After all known miRNA and other non-coding RNA sequences were extracted from the two datasets, the remaining unique small RNAs were aligned to the rhesus monkey genome assembly (rheMac2) downloaded from the UCSC genome browser. MIREAP software version 0.2 (Huada Genomics Institute Co. Ltd.) was used to predict novel miRNA candidates under default settings. A novel miRNA was considered typical only when it fulfilled three criteria: 1) mature miRNA has to be supported by a minimum of five independent sequence reads originating from at least one small RNA library; 2) the secondary structure of the hairpin is steady, with the free energy of hybridization lower than −20 kcal/mol; and 3) hairpin is located in intergenic or intronic regions.

Tag Sequencing of mRNA 3′-Termini—DpnII-tag sequencing was performed according to the protocol of Digital Gene Expression Tag Profile Kit (Illumina). Briefly, total RNAs (1 μg) were incubated with oligo-dT beads to capture the polyadenylated RNA fraction. First-strand and second-strand cDNAs

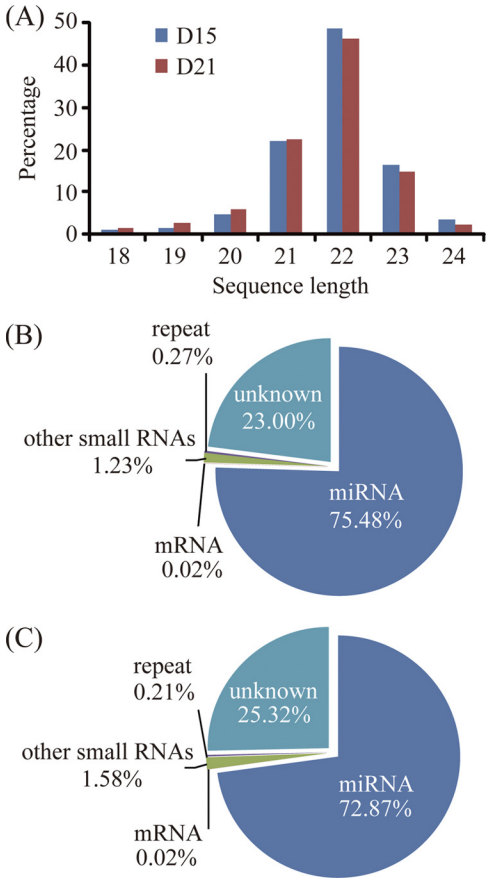

FIGURE 1. **Deep sequencing of small RNA libraries derived from the endometrium of rhesus monkey.** *A*, length distribution of small RNAs. *B* and *C*, composition of small RNA species in the endometrium on days 15 and 21 of the menstrual cycle, respectively.

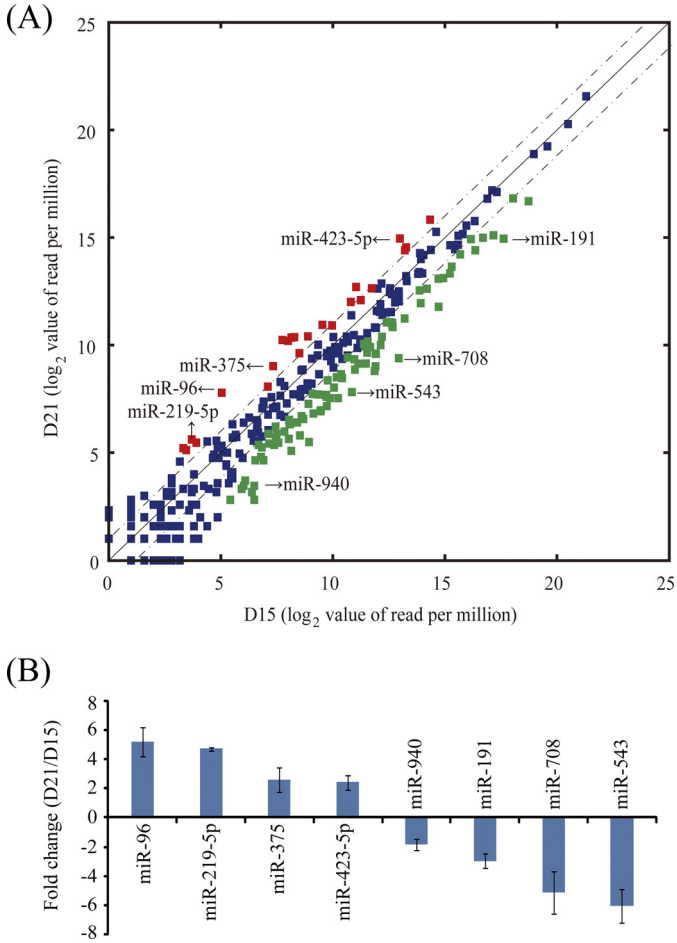

FIGURE 2. **Identification of differentially expressed miRNAs.** *A*, scatter plot represents miRNAs significantly changed at least 2-fold ($p < 0.001$). The RPM (reads per million) values are plotted in $\log_2$ scale. *Dash lines* indicate the 2-fold difference boundaries. *Red dots* indicate up-regulated miRNAs, and *green dots* represent down-regulated ones on day 21 compared with day 15. *B*, confirmation of 8 selected miRNAs by qRT-PCR analysis. Quantitative miRNA expression data were normalized to the expression levels of U6. Relative fold changes were shown as mean ± S.E.

were synthesized while the RNA was bound to the beads, and the double stranded product was digested with restriction enzyme DpnII, which cuts ~250 bp upstream of the messenger RNA poly(A) tail. The fragments that remained attached to the beads were ligated to an adapter, which contains a MmeI recognition site. The restriction enzyme MmeI was then used to cut 16 bp downstream from the recognition site, thus creating a 20 bp unique tag (including 4 bp of the DpnII recognition site). Then another adapter was ligated at the site of MmeI cleavage. The resulting sequences, containing adaptors on both 5′- and 3′-ends, were amplified using PCR and purified on PAGE gels. Finally, high throughput sequencing was carried out using the same platform as described above.

After sequencing, all of 20 bp tags were extracted and potentially erroneous tags (single copy tags or tags containing ambiguous bases "N") were filtered out. Most rhesus monkey genes have lacked annotated 3′-UTRs. In order to identify 3′-UTR sequence, tags were mapped to the rhesus monkey genome assembly (rheMac2) using the Bowtie alignment tool. Only unique mapping tags were used for further analysis. Gene annotations for rhesus monkey were downloaded from ENSEMBL release 61, and the stop codon coordinates were determined in the genome. For a given gene, tags falling into regions from 1 kb upstream to 10 kb downstream of the stop codon were considered to support the evidence of transcriptional termination. The Polyadq program (52), which scans sequences for AATAAA or ATTAAA and downstream elements typical of mammalian poly(A) signals, was used to predict putative polyadenylation sites between the matched tag and the closest DpnII (GATC) site downstream from the tag. When more than one poly(A) signals were found, only the one with the highest score was chosen. The full-length of 3′-UTR sequences were defined as the region from the stop codon to the poly(A) signal site. In the end, quantitative analysis of these tags was performed using the same statistical framework as described in the section above.

Quantitative RT-PCR for miRNA and mRNA Quantification—Quantitative RT-PCR was carried out to validate the expression levels of miRNAs determined by deep sequencing. Total RNAs were extracted using TRIzol reagent (Invitrogen), digested with DNase I and reverse-transcribed into cDNA with PrimeScript™ RT reagent kit (TaKaRa). Each reverse transcription reaction was performed in 10 μl reaction volume containing 0.1 μg of total RNAs, 2 μl of 5 × PrimeScript buffer, 250 fmol special stem-loop RT primers, and 0.5 μl of PrimeScript RT Enzyme Mix I. Reverse transcription conditions were as follows: 16 °C for 30 min, 60 cycles of 30 °C for 30 s, 42 °C for 30 s,

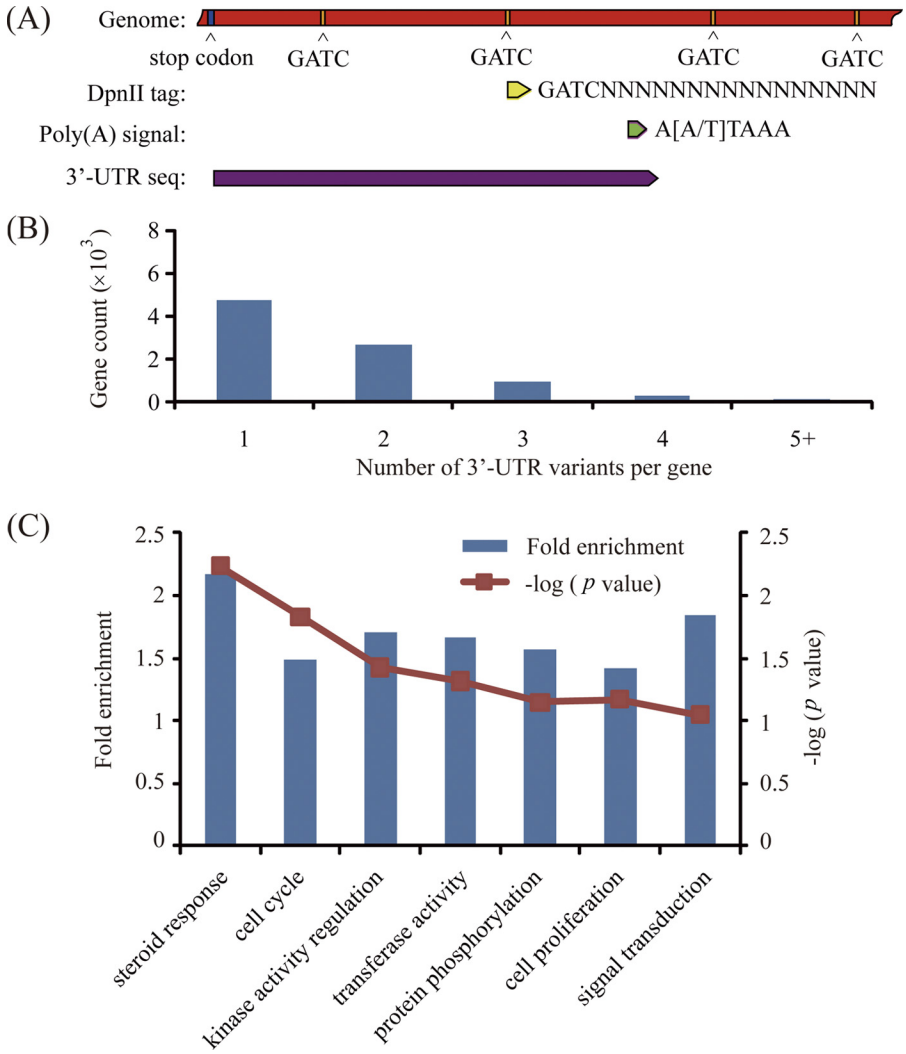

FIGURE 3. **The 3′-UTRome of the rhesus monkey endometrium.** *A*, 3′-UTRome discovery pipeline. *B*, distribution of 3′-UTR variants per gene. *C*, functional clustering and enrichment analysis of differentially expressed genes identified by tag sequencing. DAVID online tools were used for enrichment analysis. Genes were classified according to biological processes.

50 °C for 1 s, and 85 °C for 5 min. The reverse transcription products were amplified using a SYBR Premix Ex TaqTM kit (TaKaRa) on the Rotor-Gene 3000A system for 95 °C for 10 s, followed by 40 cycles of 95 °C for 5 s, 60 °C for 5 s and 72 °C for 8 s. U6 was amplified as a reference for normalization.

For mRNA and long non-coding RNA quantification, rhesus monkey *GAPDH* was selected as the internal control. For reverse transcription, 25 pmol of Oligo dT primers and 50 pmol of random 6-mer were used as RT primers in a 10 μl reaction system of PrimeScript^{TM} RT reagent kit according to the manufacturer's instructions. The cDNAs were amplified using the following PCR program: 95 °C for 10 s, 40 cycles of 95 °C for 5 s and 60 °C for 34 s. All primers used in this study were listed in supplemental Table S1.

Northern Blot—For the preparation of the probe for Northern blot, a 425 bp fragment of rhesus monkey *PGR* gene was amplified by RT-PCR. The derived fragment was cloned into pGEM-T plasmid (Promega) and verified by sequencing. The recombinant plasmid was amplified with the primers for T7 and SP6 to prepare templates for labeling sense or antisense probes, respectively. Digoxigenin (DIG)-labeled complementary RNA (cRNA) probes were transcribed *in vitro* using DIG RNA labeling kit (Roche).

Total RNAs were extracted from rhesus monkey endometrium, run on a 1% agarose gel in the presence of 2.2 M formaldehyde, transferred onto positively charged nylon membrane (Roche), and hybridized with the DIG-labeled RNA probes in DIG Easy Hyb (Roche) at 68 °C for 16 h. The membranes were washed twice for 5 min each at room temperature with 1 × SSC, 0.1% SDS, and then washed twice for 15 min each at 68 °C with 0.1 × SSC and 0.1% SDS. The hybridized bands were visualized using CDP-Star (Roche).

Western Blot—Cultured cells were collected directly in lysis buffer (50 mM Tris-HCl, pH 7.5, 150 mM NaCl, 1% Triton X-100, and 0.25% sodium deoxycholate). Protein concentration was measured with BCA Reagent kit (Applygen, Beijing, China). Samples were run on a 10% PAGE gel and transferred onto nitrocellulose membranes. After blocking in 5% nonfat dry milk in PBST (0.1% Tween 20 in PBS) for 1 h, membranes were incubated overnight at 4 °C with primary antibody for PGR (ab2764, Abcam) or β-Actin (ab8227, Abcam). After washed three times in washing buffer, membranes were incubated in

matched second antibody conjugated with horseradish peroxidase. The signals were developed with ECL Chemiluminescent kit (Amersham Biosciences, Arlington Heights, IL).

In Silico Analysis of miRNA Binding Sites—Rhesus monkey 3′-UTR sequences were scanned for perfect matches against the miRNA seed sequence (nucleotides 2~7) and the identity of one upstream and one downstream flanking nucleotides were also considered for each seed match. In this study, three types of seed match as defined in the TargetScan 5.1 algorithm (53) were allowed: 8mer (exact match to positions 2–8 of the mature microRNA followed by an *A*), 7mer-m8 (exact match to positions 2–8 of the mature microRNA), and 7mer-1A (exact match to positions 2–7 of the mature microRNA followed by an *A*). The rhesus monkey 3′-UTR boundaries were used to acquire orthologous 3′-UTRs from the 46-genome vertebrate Multiz alignments from the UCSC genome browser. The conservation of target sites was studied in the aligned sequences of commonly used model organism for studying endometrial receptivity, including human, chimpanzee, rhesus monkey, mouse, and rat.

Dual-luciferase Activity Assay—For luciferase reporter experiments, the 3′-UTR segments of rhesus monkey harboring predicted miRNA binding sites were cloned into the XbaI-FseI restriction site downstream to the firefly luciferase reporter gene of pGL3 control vector (Promega). The miRNA-binding sites were site-directed mutated using the Quick Change site-directed mutagenesis kit (Stratagene). All the clones were confirmed by sequencing.

Rhesus monkey LLC-MK2 cells were cultured in DMEM Medium (Invitrogen) with 10% fetal bovine serum (Biochrom, Berlin, Germany). Human ECC-1 cells were maintained in RPMI 1640 Medium (Sigma) with 5% fetal bovine serum (Biochrom). Mouse TM3 cells were grown in DMEM/F12 Medium (Invitrogen) with 5% horse serum (Minghai, Lanzhou, China) and 2.5% fetal bovine serum (Biochrom). All cells were preplated in 24-well tissue culture plates at a concentration of 3×10^4 cells per well. Transfection was performed the next day using Lipofectamine 2000 (Invitrogen) with 40 ng of pRL-TK, 200 ng of pGL3 vector containing the desired 3′-UTR with or without site-directed mutations, and 50 ng of desired pre-miRNA, anti-miR inhibitor or negative control (Ambion). Cell lysate was collected and assayed 30 h after transfection. The activity of firefly and *Renilla* luciferase was measured using a Dual-luciferase reporter assay system (Promega). The plasmid pRL-TK containing the *Renilla* luciferase was used for normalization of transfection efficiency. Each experiment was run in triplicate and repeated at least three different times.

RESULTS

Global Analysis of miRNA Changes Associated with Endometrial Receptivity—To address the issue of miRNAs associated with endometrial receptivity in rhesus monkey, endometrial tissues were collected on day 15 (D15, pre-receptive phase) and day 21 (D21, receptive phase) of the menstrual cycle. Through deep sequencing, we obtained 13,661,533 reads from day 15 and 12,296,254 reads from day 21, respectively. The raw data in this study were deposited in Gene Expression Omnibus database (GSE31041). Most of these reads were 18~26 nt long with a peak around 22 nt (Fig. 1*A*), demonstrating that the small RNA libraries were highly enriched in mature miRNAs. Genomic mapping of these reads showed that the predominant RNA species (based on read counts) in both libraries were miRNAs, representing 75.48% of day 15 and 72.87% of day 21, respectively. There were small amounts of other non-coding RNAs (rRNAs, tRNAs, piRNAs, snRNAs, snoRNAs, etc.), mRNAs and genomic repeats, being no more than 2% of total reads (Fig. 1, *B* and *C*). From the unknown reads perfectly mapped to genome, we identified a low-level expression of 113 potential novel miRNAs (supplemental Table S2). These miRNA candidates deserve further investigation.

We then compared the relative endometrial miRNA abundance on days 15 and 21. Read counts for each library were normalized to reads per million. Differentially expressed miRNAs were identified according to their fold changes (>2-fold) and *p* values (<0.001). Compared with day 15, 85 miRNAs were down-regulated and 22 miRNAs were up-regulated on day 21 (Fig. 2*A*). To confirm the results from miRNA deep sequencing,

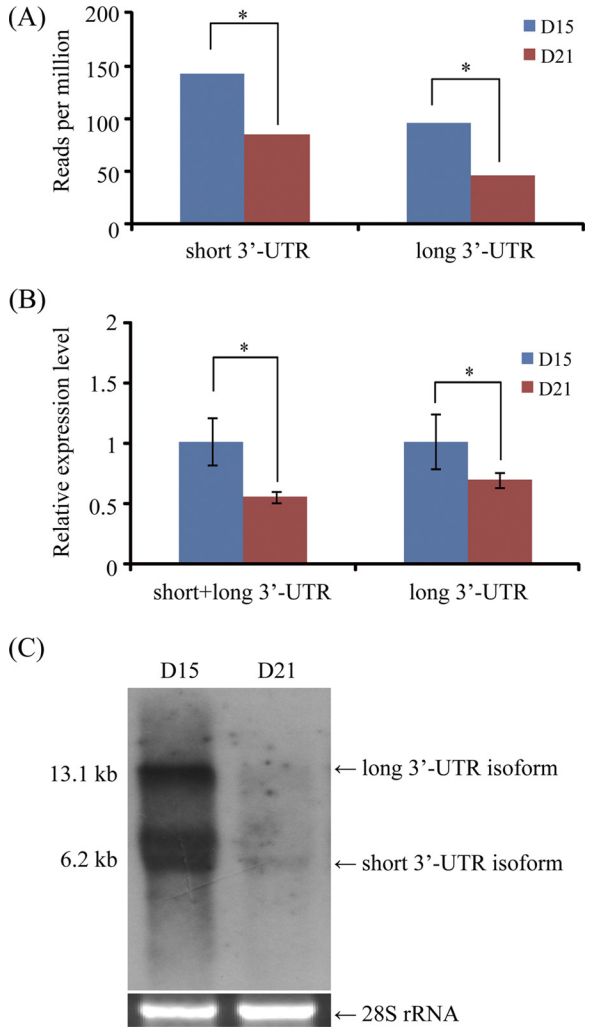

FIGURE 4. **The 3′-UTR variants of *PGR*.** *A*, expression of long and short 3′-UTR variants revealed by tag sequencing. *B*, real-time RT-PCR quantification of *PGR* 3′-UTR variants. Primers were designed in the region shared by short and long 3′-UTR variants, as well as the region specific to the long 3′-UTR variant alone. *, $p < 0.05$. *C*, confirmation of *PGR* mRNA in the endometrium of rhesus monkey by Northern blot hybridization. The 28 S rRNA was used as RNA loading control.

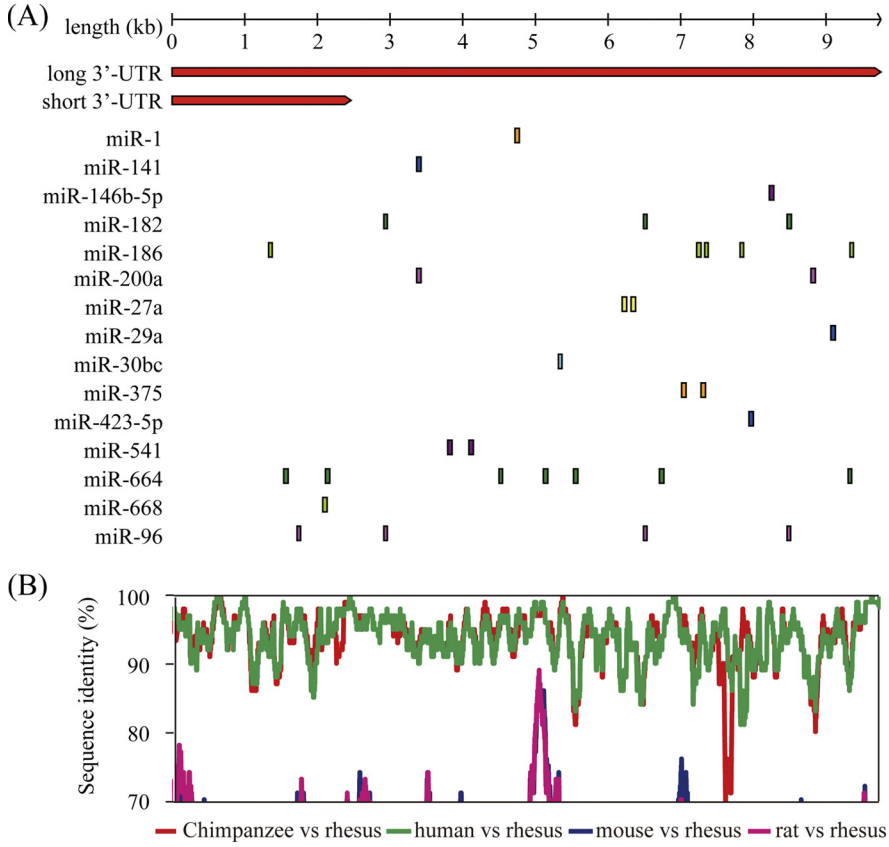

FIGURE 5. **Prediction of miRNAs targeting *PGR*.** *A*, schematic diagram of potential binding sites of miRNAs in the *PGR* 3′-UTR. A total of 34 potential sites corresponding to 15 unique miRNAs were identified. *B*, conservation of the 3′-UTR sequence. Aligned sequences corresponding to the 3′-UTR of rhesus monkey *PGR* gene were retrieved from the UCSC Genome Browser database. Pairwise conservation profile was obtained, and identity score was calculated in a 100 nt sliding window. The identity score cut-off value was set as 70%.

8 miRNAs were chosen for qRT-PCR validation according to their fold change or abundance index. The expression levels of these 8 miRNAs measured by qRT-PCR were similar to deep sequencing data (Fig. 2*B*).

The Landscape of Endometrial 3′-UTRome—MiRNAs regulate the stability and translation of target mRNAs through complimentary binding sites in their 3′-UTRs. However, the gene sequence resources for rhesus monkey are relatively limited and most of the genes have lacked annotated 3′-UTRs. To predict the target genes of miRNAs, we analyzed the 3′-UTRome of rhesus monkey endometrium through tag sequencing of mRNA 3′-termini. The tags were generated from the 3′ most recognition site of restriction enzyme DpnII, which recognizes GATC, proving transcriptional termination information for each mRNA. The polyadenylation site, which locates between the DpnII-tag and the next GATC site, was predicted using the polydq algorithm. As most 3′-UTRs have no introns (23, 24), the 3′-UTR sequences were extracted from the stop codon to the poly(A) signal site in the genome (illustrated in Fig. 3*A*). Using this method, we defined 20,149 distinct 3′-UTRs in rhesus monkey for 10,677 protein-coding genes. About 50% of the genes expressed in the rhesus monkey endometrium exhibited alternative 3′-UTRs (Fig. 3*B*). By counting the 3′-UTR sequence reads for each gene, we measured the relative expression levels of genes in the rhesus monkey endometrium. In comparison with day 15, there were 487 genes up-regulated and 453 genes down-regulated at least 2-fold ($p < 0.001$) on day 21 (supplemental Table S3). Based on Gene Ontology analysis, the genes involved in steroid response were highly enriched (Fig. 3*C*), in agreement with the idea that steroid hormones are key regulators of endometrial receptivity (26, 27).

Characterization of Progesterone Receptor 3′-UTR—Among these steroid response-related genes, we focused on the progesterone receptor (*PGR*), because *PGR* is a key component of progesterone signaling and is necessary for embryo implantation (28, 29). Interestingly, we identified two tags falling into the 3′-UTR region of *PGR*. One is 5′-GATCATGGATTTTAACGGTA-3′, which represents a long 3′-UTR of 9,398 nt in length. The other is 5′-GATCTCTGTCTGCAATGTAG-3′, corresponding to a short 3′-UTR of 2,482 nt. According to tag abundance, both long and short 3′-UTRs were significantly decreased on day 21 compared with day 15 (Fig. 4*A*). The existence of these 2 isoforms was confirmed by qRT-PCR (Fig. 4*B*) and Northern blot (Fig. 4*C*).

The coding sequence (CDS) of *PGR* is conserved among mammals (30). To further address the question of whether the 3′-UTR sequences of *PGR* are also conserved, we used the BLAST tool to search the gene database for matches. Close matches were found only in the human but not in other mammals. The long 3′-UTR is homologous to human *PGR* (NM_000926.4). As the 3′-UTR annotation for genes may be incomplete, we next retrieved the sequences corresponding to the 3′-UTRs of *PGR* aligned by Multiz against 5 representative mammals (rhesus monkey, human, chimpanzee, mouse, and

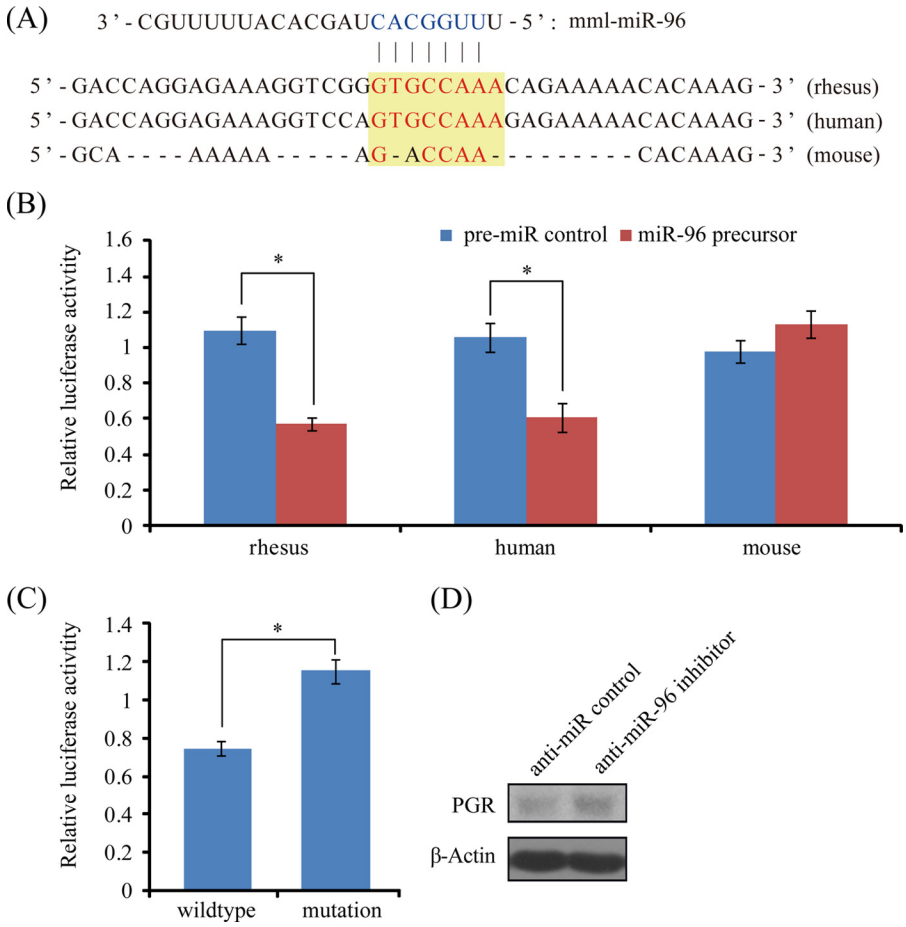

FIGURE 6. **MiR-96 regulation on *PGR*.** *A*, sequences of predicted *miR-96* binding site in the 3′-UTR of *PGR*. Sequence conservation was compared among rhesus monkey, human, and mouse. The seed sequence of *miR-96* was colored in *blue* and the seed-complementary sequence in the 3′-UTR of *PGR* is indicated in *red*. *B*, target validation by luciferase assay in three different species. The 3′-UTR fragments derived from rhesus monkey, human, and mouse were cloned and subjected to luciferase assay in rhesus LLC-MK2 cells, human ECC-1 cells and mouse TM3 cells, respectively. *C*, point mutation analysis of *miR-96* seed binding sequence. The seed binding site (GTGCCAAA) was mutated into GACCAACA (to mimic the seed binding sequence in mouse). Cells were co-transfected with *miR-96* precursor. *D*, Western blot analysis of PGR-A protein expression after a transfection of anti-*miR-96* inhibitor or negative control in rhesus LLC-MK2 cells.

rat) from the UCSC Genome Browser database. Pair-wise conservation profile was obtained and identity score was calculated in a 100 bp sliding window. Using a cutoff of 70% identity, we found that the 3′-UTR of *PGR* is conserved in primates, but not in rodents (Fig. 5*B*), suggesting a species-biased miRNA binding pattern.

Because miRNAs are negative regulators of gene expression, we hypothesized that miRNAs up-regulated in the receptive endometrium may involve in the down-regulation of *PGR*. We screened the 3′-UTR sequence of *PGR* for miRNA binding sites using the seed-match algorithm. A total of 34 potential sites corresponding to 15 unique miRNAs were identified (Fig. 5*A*). Among these sites, 7 sites were rhesus monkey-specific, and 26 sites were conserved only in primates. The *miR-1* site was the only one conserved between primates and rodents. However, the 3′-UTR of *PGR* is only 3,473 bp long (RefSeq: NM_008829.2, in agreement with Northern blot results from a previous study (31)) and the *miR-1* binding site was out of the 3′-UTR range in the mouse. Thus, it is not a conserved site in the mRNA level between primates and rodents.

MiRNA Regulation on PGR through Non-conserved miRNA Binding Sites in the 3′-UTR—MiR-96 is highly conserved among mammals (32). It was up-regulated in the rhesus monkey endometrium on day 21 compared with day 15. According to the bioinformatic predictions, there were 4 potential *miR-96* binding sites in the 3′-UTR of *PGR*. Luciferase reporter assay was used to validate these sites. The 3′-UTR fragments of rhesus monkey *PGR* spanning each *miR-96* binding site were cloned downstream to a firefly luciferase gene. In LLC-MK2 cells, a significant decrease of firefly luciferase activity was observed in the forth construct, containing the binding site located at position 8,817∼8,825 (364 bp) in the 3′-UTR of *PGR* (Fig. 6, *A* and *B*). To further test the direct binding of this site to *miR-96*, we introduced point mutations into the seed binding sequence. The reduction of luciferase reporter was eliminated by mutations (Fig. 6*C*). Then the orthologous target sites in other species were retrieved from UCSC Multiz genome alignment. In the human, this site is the same as rhesus monkey, whereas 3 mismatches were found in the mouse. We tested the responsiveness of the human and mouse sequences to *miR-96* with luciferase reporter assay. The 3′-UTR fragment homologs from human and mouse were cloned and assayed luciferase activity. As expected, *miR-96* mediated regulation on *PGR* 3′-UTR was retained in humans, but lost in mice (Fig. 6*B*). Finally, we checked *miR-96* regulation of endogenous PGR protein expression using antisense inhibitor. In rhesus LLC-MK2

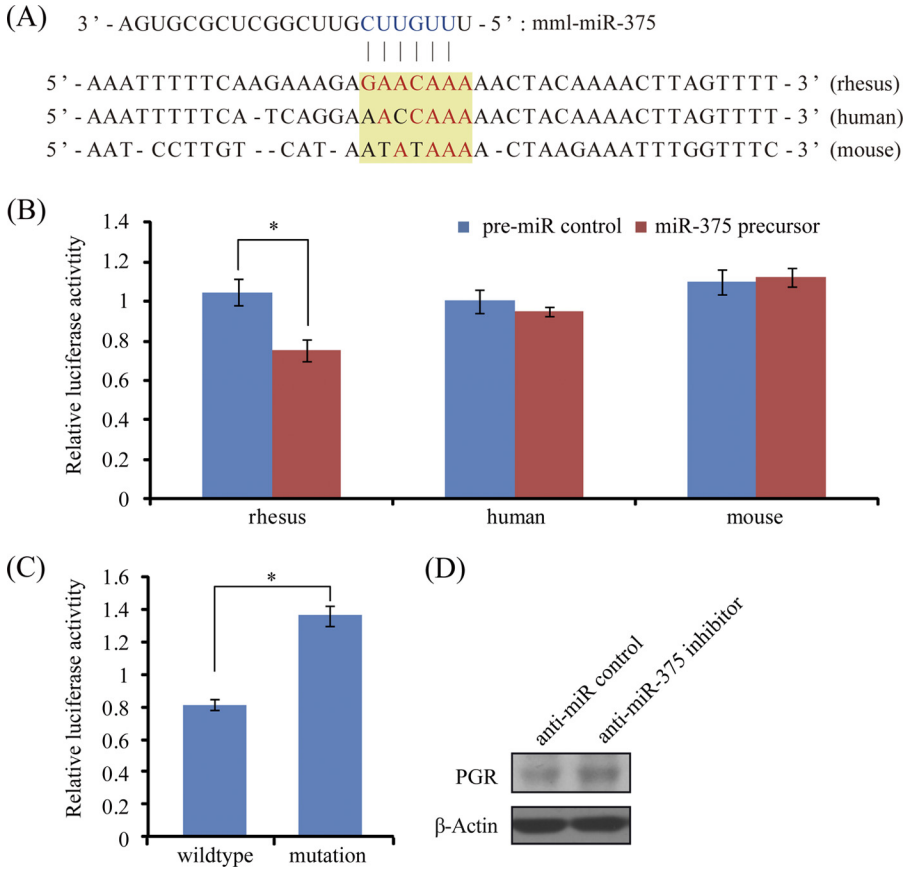

FIGURE 7. **MiR-375 regulation on *PGR*.** *A*, sequences of predicted *miR-375* binding site in the 3′-UTR of *PGR*. *B*, target validation by luciferase assay in three different species. *C*, point mutation analysis of *miR-375* seed binding sequence. The seed binding site (GAACAAA) was mutated into AACCAAA (to mimic the seed binding sequence in human). Cells were co-transfected with *miR-375* precursor. *D*, Western blot analysis of PGR-A protein expression after a transfection of anti-*miR-375* inhibitor or negative control in rhesus LLC-MK2 cells.

cells, PGR-A protein level was induced upon anti-miR-96 inhibitor treatment (Fig. 6*D*). Collectively, our results indicate that *PGR* is a valid target of *miR-96* in rhesus monkey and human, but not in rodents.

Like *miR-96*, *miR-375* is conserved in most mammals (33). It was also up-regulated in the receptive endometrium in our study. *MiR-375* was predicted to target *PGR* on 2 sites. Using luciferase reporter assay, we showed that only the second site was functional. This site was located at position 7,309∼7,315 (570 bp) in the 3′-UTR of *PGR* (Fig. 7, *A* and *B*). Introduction of point mutations into the predicted seed binding sequence abrogated miR-375 repression of luciferase reporter (Fig. 7*C*). Evolutionary analysis showed that the binding site is rhesus monkey-specific. There were 2∼3 mismatches in human and mouse. Further luciferase reporter assay showed that *PGR* 3′-UTR fragments derived from human and mouse escaped miR-375 regulation (Fig. 7*B*). Consistently, anti-miR-375 inhibitor was able to elevate endogenous PGR-A protein level in rhesus LLC-MK2 cells (Fig. 7*D*). Thus, the *miR-375* regulation on *PGR* was rhesus monkey-specific.

MiR-219–5p Regulation on a Long Non-coding RNA Immediately Downstream of the PGR Locus—In our sequencing data, we found a tag (5′-GATCATTTGGCCATGAAAAT-3′) from an unknown transcript. This tag was located in the intergenic region immediately downstream of *PGR* (Fig. 8*A*). Using RT-PCR and primer sets spanning the upstream and downstream of this transcript, we confirmed that this transcript was an independent transcript rather than another *PGR* variant generated by 3′-UTR extension (Fig. 8*B*). This transcript was classified as a long non-coding RNA (lncRNA) using the Coding Potential Calculator (CPC) tool version 0.9r2 (54). By searching the transcript data base, we found that it was highly homologous to a human non-coding RNA, which was characterized as a *cis*-regulator of *PGR* (34). No matches were found in non-primate mammals, implying that this long non-coding RNA was primate-specific. We designated this lncRNA as *lncRNA-PGR-3p*. Like *PGR*, *lncRNA-PGR-3p* was also down-regulated on day 21 compared with day 15.

Previous studies have indicated that lncRNAs are valid targets for miRNAs (35–37). We then predicted the miRNAs that have potential binding sites on *lncRNA-PGR-3p*. A candidate, *miR-219–5p*, one of the up-regulated miRNAs in the receptive endometrium, was selected (Fig. 9*A*). *MiR-219–5p* had no predicted binding sites in the 5′-UTR, CDS, or 3′-UTR of *PGR*. In order to examine the interaction between *lncRNA-PGR-3p* and *miR-219–5p*, we cloned a 485 bp fragment of *lncRNA-PGR-3p* containing the putative miRNA binding site into the luciferase reporter vector. Luciferase assay and following point mutation analysis confirmed that *lncRNA-PGR-3p* was genuinely targeted by *miR-219–5p* in primates (Fig. 9, *B* and *C*).

To test whether *lncRNA-PGR-3p* could regulate PGR expression in rhesus LLC-MK2 cells, *lncRNA-PGR-3p* RNAi was per-

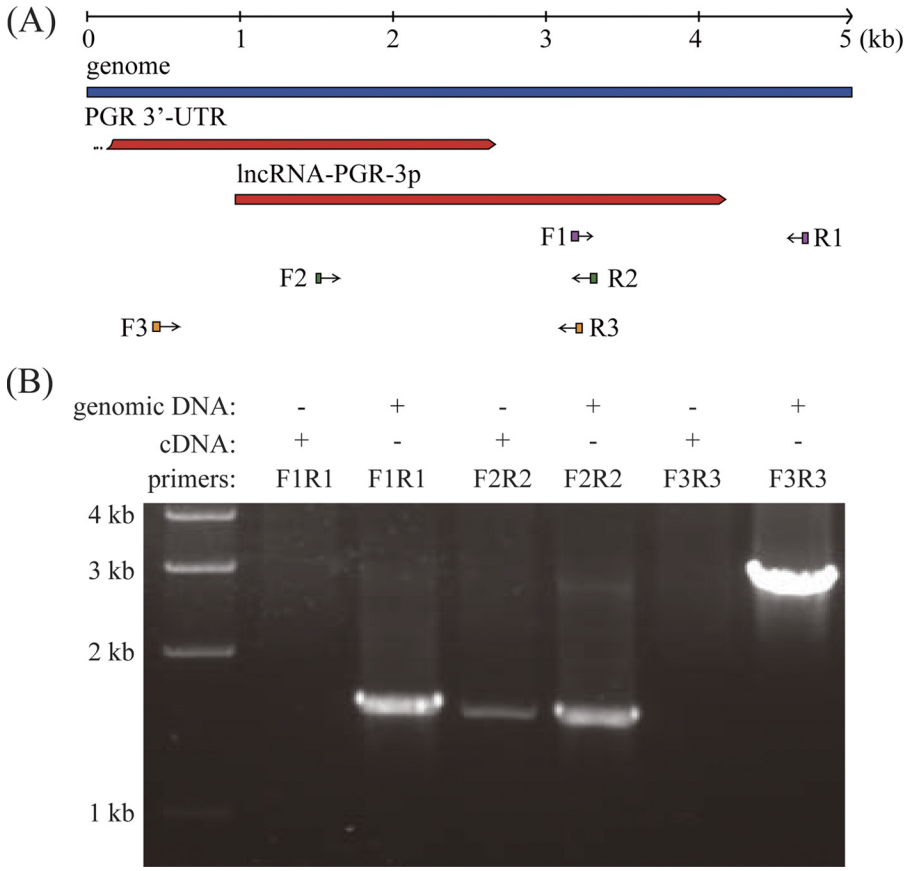

FIGURE 8. **Characterization of a long non-coding RNA, *lncRNA-PGR-3p*.** *A*, genomic location of *lncRNA-PGR-3p* and primers used for RT-PCR. *B*, agarose gel analysis of RT-PCR amplification products. The amplification of genomic DNA was included as a positive control for primer design. RT-PCR with primers F2 and R2 revealed a novel transcript immediately downstream of the *PGR* gene locus. No transcript was detected from primers F1 and R1 or from primers F3 and R3, even though these primer sets could amplify genomic DNA efficiently.

formed. After cells were transfected with designed siRNA, *lncRNA-PGR-3p* expression level was confirmed by qRT-PCR (Fig. 9*D*). With *lncRNA-PGR-3p* expression level reduced to about 60% by RNAi, PGR-A protein expression was repressed (Fig. 9*E*), suggesting that *lncRNA-PGR-3p* was a positive regulator of PGR in rhesus LLC-MK2 cells.

Because *lncRNA-PGR-3p* is a target of *miR-219–5p* and also a regulator of *PGR*, we assumed that *miR-219–5p* may exert its regulation on *PGR* expression through *lncRNA-PGR-3p*. To confirm this, LLC-MK2 cells were transfected with the *miR-219–5p* antisense inhibitor. Compared with the control, the level of PGR-A protein was up-regulated after cells were transfected with anti-miR-219-5p inhibitor (Fig. 9*F*). Additionally, *miR-219-5p* down-regulation on PGR luciferase activity was abrogated when rhesus LLC-MK2 cells were co-transfected with *lncRNA-PGR-3p* siRNA (Fig. 9*G*). Our data indicated that *miR-219-5p* is potentially an indirect regulator of *PGR* expression through *lncRNA-PGR-3p*.

DISCUSSION

In this study, deep sequencing was applied to determine the miRNA expression profiles in the endometrium of rhesus monkey. We detected 325 known miRNAs along with 113 potential novel miRNAs that had not been reported in any species before. Although 89.3% of known miRNAs are conserved in primates and rodents, 11.5% of potential novel miRNAs are conserved according to genomic sequence alignments. Most of them are primate-specific. All these novel miRNAs were expressed at very low levels in the endometrium. Therefore, it seems that the conserved known miRNAs are the major players in the endometrium, and the roles of novel miRNAs were not pursued further.

In this study, two *PGR* variants with different 3′-UTR sequences were identified in the endometrium of rhesus monkey. Both of them were significantly down-regulated in receptive endometrium. These two variants were different from the well known *PGR-A* and *PGR-B* variants that result from the usage of different transcription start sites (38, 39). Previous studies have shown that alternative 3′-UTRs in varying length caused by alternative polyadenylation are frequent in mammals, often differentially expressed in a tissue- and phase-specific manner (22). The long and short 3′-UTRs are different substrates for miRNA regulation. Genes that prefer to increase the relative abundance of short 3′-UTR isoforms in receptive endometrium might be due to the need to escape miRNA regulation through evolutional selection when particularly high levels of gene products are needed. On the other hand, genes that choose to express a higher relative abundance of long 3′-UTR isoforms might provide additional regulatory interfaces that mediate the interactions with miRNAs at selected spatiotemporal coordinates. The existence of isoform prefer-

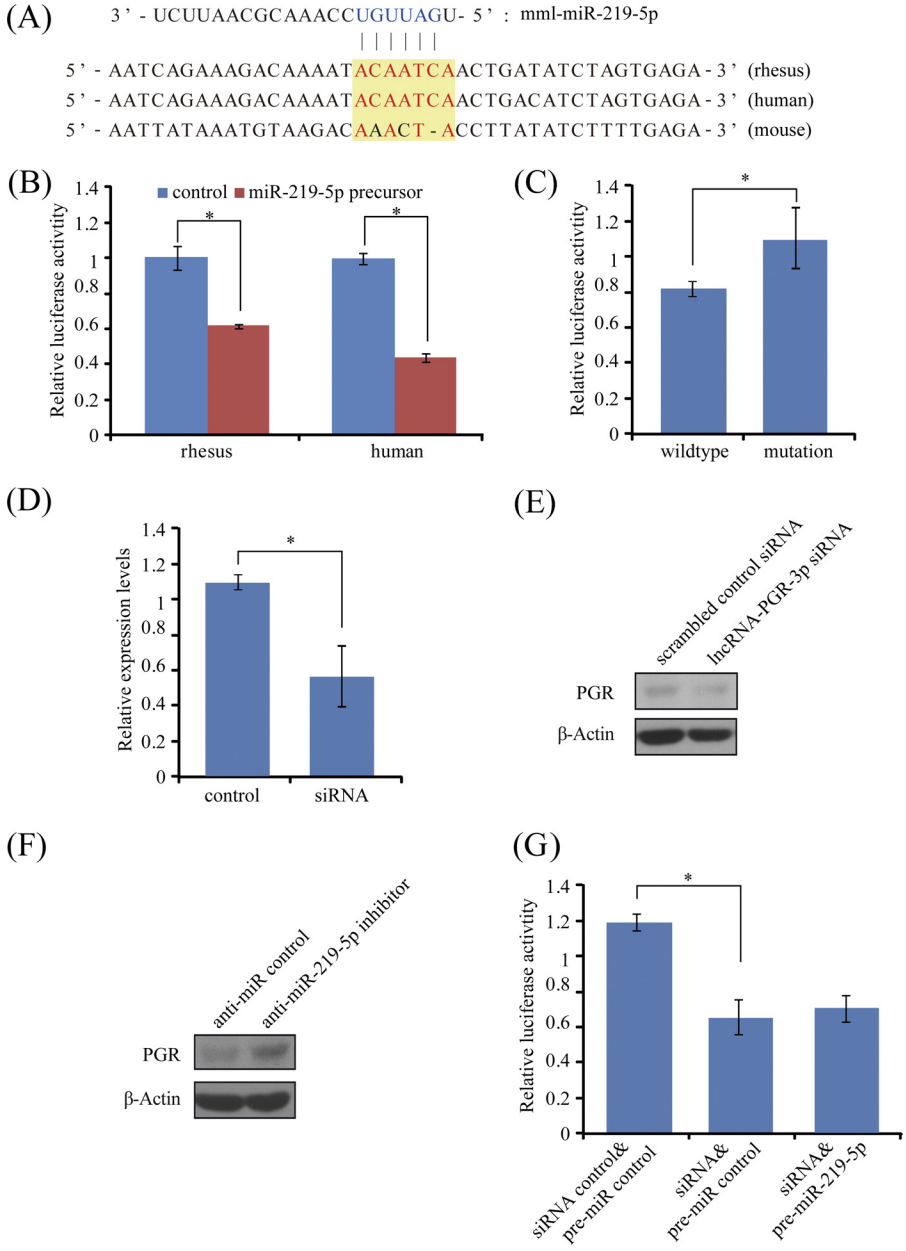

FIGURE 9. **MiR-219–5p regulation on *PGR* via *lncRNA-PGR-3p*.** *A*, sequences of predicted *miR-219–5p* binding site in the *lncRNA-PGR-3p* non-coding RNA. *B*, target validation by luciferase assay in rhesus monkey and human. The 3′-UTR fragments derived from rhesus monkey and human were cloned and subjected to luciferase assay in rhesus LLC-MK2 cells and human ECC-1 cells, respectively. *C*, point mutation analysis of *miR-219–5p* seed binding sequence. The seed binding site (ACAATCA) was mutated into AAACTAC. Cells were co-transfected with *miR-219–5p* precursor. *D*, efficiency of *lncRNA-PGR-3p* RNAi on *lncRNA-PGR-3p* RNA level determined by qRT-PCR. The siRNA sequence designed for rhesus *lncRNA-PGR-3p* was 5′-GCUGUAAGUUUGAGUUGAUdTdT-3′. *E*, Western blot analysis of PGR-A protein expression after rhesus LLC-MK2 cells were treated with *lncRNA-PGR-3p* siRNA. *F*, level of endogenous PGR-A protein measured by Western blot after rhesus LLC-MK2 cells were transfected with the anti-miR-219-5p inhibitor or control. *G*, indirect regulation of *PGR* by *miR-219-5p via lncRNA-PGR-3p*. When rhesus LLC-MK2 cells were co-transfected with *lncRNA-PGR-3p* siRNA, *miR-219–5p* down-regulation on PGR luciferase activity was abrogated.

ences adds another layer of complexity in miRNA-mediated post-transcriptional regulation.

Using bioinformatic tools, we found that the 8 qRT-PCR-validated miRNAs in this study potentially targeted 492 genes. Functional classification analysis indicated that genes responsible for steroid response were highly enriched (data not shown). Among these steroid response genes, we focused on the *PGR* gene, a key component of the progesterone signaling. It has been established that *PGR* is indispensable for endometrial receptivity and embryo implantation (28, 29). Paradoxically, *PGR* is repressed in receptive endometrium in most mammals. In humans, the retention of *PGR* expression in endometrial epithelium is associated with embryo implantation failure. Loss of the *PGR* in the luminal epithelium is concomitant with the decrease of mucin glycoprotein 1 (*MUC-1*), an inhibitor of blastocyst implantation (40, 41). It is notable that *MUC-1* remains

abundant at the luminal epithelial surface during the receptive phase in humans, in contrast to other primates (42). This phenomenon is thought to be an evolutionary advantage to sort out defective embryos prior to implantation by the continued *MUC-1* barrier. The loss of epithelial *PGR* also provides the opportunity for stromal cells to exercise a paracrine-mediated effect on epithelial $\alpha v\beta 3$ integrin expression (43). However, little is known about how *PGR* is down-regulated. It has been reported that *miR-26a* and *miR-181a* target PGR and repress PGR expression in human MCF7 cells (44). However, no change in *miR-26a* or *miR-181a* expression was observed in the receptive endometrium in this study, demonstrating the down-regulation of PGR is not linked to *miR-26a* or *miR-181a*. In this study, we showed that both *miR-96* and *miR-375* act as direct negative regulators on the long 3′-UTR *PGR* isoform. These miRNAs may fine-tune the dosage of PGR signaling and contribute to endometrial receptivity. Noticeably, the short 3′-UTR *PGR* isoform escapes the regulation by these two miRNAs.

Despite the evolutionary conservation of most miRNAs, the 3′-UTR sequences of *PGR* are poorly conserved between primates and rodents. Consequently, all predicted miRNA binding sites in the 3′-UTR of *PGR* were rhesus monkey-specific or only conserved in primates. However, the lack of conservation does not necessarily mean lack of function. Using luciferase assay, we confirmed that *PGR* is a primate-specific target of *miR-96* and a rhesus monkey-specific target of *miR-375*, respectively. Previously, Rosa *et al.* have shown that the *miR-430/427/302* family of miRNAs have a distinct effect on Nodal signaling during mesendoderm differentiation in African frog and human (45), indicating a species-specific bias of miRNA target selection. To date, most algorithms for target prediction are limited to predicting evolutionarily conserved candidate target sites, while non-conserved targets are completely missed. It is reported that evolutionary conserved sites are more reliable than non-conserved ones, based on the hypothesis that the 3′-UTR sequences are under selective pressure to maintain miRNA binding sites, and these sites should be more conserved than random sequences (46). In this study, we tested 6 poorly conserved miRNA binding sites (4 for *miR-96* and 2 for *miR-375*) using luciferase assay, 2 of which were proved functional. The false positive rate was 67%, higher than that for conserved miRNA-binding site (22∼31%) (47). In the whole 3′-UTRome scale, more than 75% of predicted miRNA binding sites were poorly conserved. Therefore, the number of functional poorly conserved sites is estimated to be very large, probably close to that of conserved sites. We believe that these widespread poorly conserved miRNA binding sites may help shape the species-specific characteristics of endometrial receptivity in the rhesus monkey and the primate order as well.

Recently, there are an increasing number of reports describing mRNA-like lncRNAs (48). Studies have indicated that some of these lncRNAs also harbor miRNA binding sites, just like protein-coding mRNAs (35–37). In this study, we identified an lncRNA, *lncRNA-PGR-3p*, immediately downstream of *PGR*. It was highly homologous to a known non-coding RNA in human, which was found to modulate the expression of *PGR* upon exogenous siRNA delivery (34). We discovered that *lncRNA-PGR-3p* was directly targeted by *miR-219-5*p. In rhesus LLC-MK2 cells, *miR-219-5p* was capable to repress *PGR* expression efficiently via *lncRNA-PGR-3p*. Because no other protein coding genes are affected, the regulation of *PGR* by *miR-219-5p* is highly specific. The regulation of *PGR* by *miR-219-5p* is species-dependent, as the sequence of *lncRNA-PGR-3p* is primate-specific. Actually, most lncRNAs are as poorly conserved as the intronic regions and less conserved than the 3′-UTR regions of protein coding genes (49, 50). MiRNA regulation through lncRNAs may represent an additional mechanism for species-specific miRNA target recognition.

Altogether, we defined the microRNome and 3′-UTRome in the receptive endometrium of rhesus monkey in this study. Through data mining, we revealed that the *PGR* gene expression is negatively modulated by miRNAs in a species-specific manner. Our study provides new insights into the species-biased molecular mechanisms underlying endometrial receptivity from the aspects of miRNA-mediated regulation.

REFERENCES

1. O'Malley, B. W., and Tsai, M. J. (1992) Molecular pathways of steroid receptor action. *Biol. Reprod.* **46,** 163–167
2. Gidley-Baird, A. A. (1981) Endocrine control of implantation and delayed implantation in rats and mice. *J. Reprod. Fertil. Suppl.* **29,** 97–109
3. de Ziegler, D., Bergeron, C., Cornel, C., Medalie, D. A., Massai, M. R., Milgrom, E., Frydman, R., and Bouchard, P. (1992) Effects of luteal estradiol on the secretory transformation of human endometrium and plasma gonadotropins. *J. Clin. Endocrinol. Metab.* **74,** 322–331
4. Ghosh, D., De, P., and Sengupta, J. (1994) Luteal phase ovarian oestrogen is not essential for implantation and maintenance of pregnancy from surrogate embryo transfer in the rhesus monkey. *Hum. Reprod.* **9,** 629–637
5. Nilsen, T. W. (2007) Mechanisms of microRNA-mediated gene regulation in animal cells. *Trends Genet.* **23,** 243–249
6. Friedman, R. C., Farh, K. K., Burge, C. B., and Bartel, D. P. (2009) Most mammalian mRNAs are conserved targets of microRNAs. *Genome Res.* **19,** 92–105
7. Gonzalez, G., and Behringer, R. R. (2009) Dicer is required for female reproductive tract development and fertility in the mouse. *Mol. Reprod. Dev.* **76,** 678–688
8. Nagaraja, A. K., Andreu-Vieyra, C., Franco, H. L., Ma, L., Chen, R., Han, D. Y., Zhu, H., Agno, J. E., Gunaratne, P. H., DeMayo, F. J., and Matzuk, M. M. (2008) Deletion of Dicer in somatic cells of the female reproductive tract causes sterility. *Mol. Endocrinol.* **22,** 2336–2352
9. Hong, X., Luense, L. J., McGinnis, L. K., Nothnick, W. B., and Christenson, L. K. (2008) Dicer1 is essential for female fertility and normal development of the female reproductive system. *Endocrinology* **149,** 6207–6212
10. Nothnick, W. B., and Healy, C. (2010) Estrogen induces distinct patterns of microRNA expression within the mouse uterus. *Reprod. Sci.* **17,** 987–994
11. Qian, K., Hu, L., Chen, H., Li, H., Liu, N., Li, Y., Ai, J., Zhu, G., Tang, Z., and Zhang, H. (2009) Hsa-miR-222 is involved in differentiation of endometrial stromal cells *in vitro*. *Endocrinology* **150,** 4734–4743
12. Kuokkanen, S., Chen, B., Ojalvo, L., Benard, L., Santoro, N., and Pollard, J. W. (2010) Genomic profiling of microRNAs and messenger RNAs reveals hormonal regulation in microRNA expression in human endometrium. *Biol. Reprod.* **82,** 791–801
13. Hu, S. J., Ren, G., Liu, J. L., Zhao, Z. A., Yu, Y. S., Su, R. W., Ma, X. H., Ni, H., Lei, W., and Yang, Z. M. (2008) MicroRNA expression and regulation in mouse uterus during embryo implantation. *J. Biol. Chem.* **283,** 23473–23484
14. Chakrabarty, A., Tranguch, S., Daikoku, T., Jensen, K., Furneaux, H., and Dey, S. K. (2007) MicroRNA regulation of cyclooxygenase-2 during embryo implantation. *Proc. Natl. Acad. Sci. U.S.A.* **104,** 15144–15149
15. Dey, S. K., Lim, H., Das, S. K., Reese, J., Paria, B. C., Daikoku, T., and Wang, H. (2004) Molecular cues to implantation. *Endocr. Rev.* **25,** 341–373

16. Wang, H., and Dey, S. K. (2006) Roadmap to embryo implantation: clues from mouse models. *Nat. Rev. Genet.* **7,** 185–199
17. Liao, B. Y., and Zhang, J. (2008) Null mutations in human and mouse orthologs frequently result in different phenotypes. *Proc. Natl. Acad. Sci. U.S.A.* **105,** 6987–6992
18. Lee, K. Y., and DeMayo, F. J. (2004) Animal models of implantation. *Reproduction* **128,** 679–695
19. Brameier, M. (2010) Genome-wide comparative analysis of microRNAs in three non-human primates. *BMC Res. Notes* **3,** 64
20. Creighton, C. J., Reid, J. G., and Gunaratne, P. H. (2009) Expression profiling of microRNAs by deep sequencing. *Brief Bioinform.* **10,** 490–497
21. Creighton, C. J., Benham, A. L., Zhu, H., Khan, M. F., Reid, J. G., Nagaraja, A. K., Fountain, M. D., Dziadek, O., Han, D., Ma, L., Kim, J., Hawkins, S. M., Anderson, M. L., Matzuk, M. M., and Gunaratne, P. H. (2010) Discovery of novel microRNAs in female reproductive tract using next generation sequencing. *PLoS One* **5,** e9637
22. Ji, Z., Lee, J. Y., Pan, Z., Jiang, B., and Tian, B. (2009) Progressive lengthening of 3′-untranslated regions of mRNAs by alternative polyadenylation during mouse embryonic development. *Proc. Natl. Acad. Sci. U.S.A.* **106,** 7028–7033
23. Mangone, M., Manoharan, A. P., Thierry-Mieg, D., Thierry-Mieg, J., Han, T., Mackowiak, S. D., Mis, E., Zegar, C., Gutwein, M. R., Khivansara, V., Attie, O., Chen, K., Salehi-Ashtiani, K., Vidal, M., Harkins, T. T., Bouffard, P., Suzuki, Y., Sugano, S., Kohara, Y., Rajewsky, N., Piano, F., Gunsalus, K. C., and Kim, J. K. (2010) The landscape of *C. elegans* 3′-UTRs. *Science* **329,** 432–435
24. Jan, C. H., Friedman, R. C., Ruby, J. G., and Bartel, D. P. (2011) Formation, regulation, and evolution of *Caenorhabditis elegans* 3′-UTRs. *Nature* **469,** 97–101
25. Pauerstein, C. J., Eddy, C. A., Croxatto, H. D., Hess, R., Siler-Khodr, T. M., and Croxatto, H. B. (1978) Temporal relationships of estrogen, progesterone, and luteinizing hormone levels to ovulation in women and infrahuman primates. *Am. J. Obstet. Gynecol.* **130,** 876–886
26. Critchley, H. O., and Saunders, P. T. (2009) Hormone receptor dynamics in a receptive human endometrium. *Reprod. Sci.* **16,** 191–199
27. Spencer, T. E., and Bazer, F. W. (2002) Biology of progesterone action during pregnancy recognition and maintenance of pregnancy. *Front. Biosci.* **7,** d1879–1898
28. Conneely, O. M., Mulac-Jericevic, B., Lydon, J. P., and De Mayo, F. J. (2001) Reproductive functions of the progesterone receptor isoforms: lessons from knock-out mice. *Mol. Cell Endocrinol.* **179,** 97–103
29. Ho, P. C. (2001) Mifepristone: a potential postcoital contraceptive. *Expert Opin. Pharmacother.* **2,** 1383–1388
30. Thornton, J. W. (2001) Evolution of vertebrate steroid receptors from an ancestral estrogen receptor by ligand exploitation and serial genome expansions. *Proc. Natl. Acad. Sci. U.S.A.* **98,** 5671–5676
31. Tan, J., Paria, B. C., Dey, S. K., and Das, S. K. (1999) Differential uterine expression of estrogen and progesterone receptors correlates with uterine preparation for implantation and decidualization in the mouse. *Endocrinology* **140,** 5310–5321
32. Jensen, K. P., and Covault, J. (2011) Human miR-1271 is a miR-96 paralog with distinct non-conserved brain expression pattern. *Nucleic Acids Res.* **39,** 701–711
33. Kloosterman, W. P., Lagendijk, A. K., Ketting, R. F., Moulton, J. D., and Plasterk, R. H. (2007) Targeted inhibition of miRNA maturation with morpholinos reveals a role for miR-375 in pancreatic islet development. *PLoS Biol.* **5,** e203
34. Yue, X., Schwartz, J. C., Chu, Y., Younger, S. T., Gagnon, K. T., Elbashir, S., Janowski, B. A., and Corey, D. R. (2010) Transcriptional regulation by small RNAs at sequences downstream from 3′ gene termini. *Nat. Chem. Biol.* **6,** 621–629
35. Wang, J., Liu, X., Wu, H., Ni, P., Gu, Z., Qiao, Y., Chen, N., Sun, F., and Fan, Q. (2010) CREB up-regulates long non-coding RNA, HULC expression through interaction with microRNA-372 in liver cancer. *Nucleic Acids Res.* **38,** 5366–5383
36. Forrest, A. R., Kanamori-Katayama, M., Tomaru, Y., Lassmann, T., Ninomiya, N., Takahashi, Y., de Hoon, M. J., Kubosaki, A., Kaiho, A., Suzuki, M., Yasuda, J., Kawai, J., Hayashizaki, Y., Hume, D. A., and Suzuki, H. (2010) Induction of microRNAs, mir-155, mir-222, mir-424, and mir-503, promotes monocytic differentiation through combinatorial regulation. *Leukemia* **24,** 460–466
37. Poliseno, L., Salmena, L., Zhang, J., Carver, B., Haveman, W. J., and Pandolfi, P. P. (2010) A coding-independent function of gene and pseudogene mRNAs regulates tumour biology. *Nature* **465,** 1033–1038
38. Meyer, M. E., Quirin-Stricker, C., Lerouge, T., Bocquel, M. T., and Gronemeyer, H. (1992) A limiting factor mediates the differential activation of promoters by the human progesterone receptor isoforms. *J. Biol. Chem.* **267,** 10882–10887
39. Wen, D. X., Xu, Y. F., Mais, D. E., Goldman, M. E., and McDonnell, D. P. (1994) The A and B isoforms of the human progesterone receptor operate through distinct signaling pathways within target cells. *Mol. Cell Biol.* **14,** 8356–8364
40. Horne, A. W., Lalani, E. N., Margara, R. A., Ryder, T. A., Mobberley, M. A., and White, J. O. (2005) The expression pattern of MUC1 glycoforms and other biomarkers of endometrial receptivity in fertile and infertile women. *Mol. Reprod. Dev.* **72,** 216–229
41. Julian, J., Enders, A. C., Fazleabas, A. T., and Carson, D. D. (2005) Compartmental distinctions in uterine Muc-1 expression during early pregnancy in cynomolgous macaque (*Macaca fascicularis*) and baboon (*Papio anubis*). *Hum. Reprod.* **20,** 1493–1503
42. Aplin, J. D. (1999) MUC-1 glycosylation in endometrium: possible roles of the apical glycocalyx at implantation. *Hum. Reprod.* **14,** (Suppl. 2), 17–25
43. Palomino, W. A., Fuentes, A., González, R. R., Gabler, F., Boric, M. A., Vega, M., and Devoto, L. (2005) Differential expression of endometrial integrins and progesterone receptor during the window of implantation in normo-ovulatory women treated with clomiphene citrate. *Fertil. Steril.* **83,** 587–593
44. Maillot, G., Lacroix-Triki, M., Pierredon, S., Gratadou, L., Schmidt, S., Bènés, V., Roché, H., Dalenc, F., Auboeuf, D., Millevoi, S., and Vagner, S. (2009) Widespread estrogen-dependent repression of micrornas involved in breast tumor cell growth. *Cancer Res.* **69,** 8332–8340
45. Rosa, A., Spagnoli, F. M., and Brivanlou, A. H. (2009) The miR-430/427/302 family controls mesendodermal fate specification via species-specific target selection. *Dev. Cell* **16,** 517–527
46. Rajewsky, N. (2006) MicroRNA target predictions in animals. *Nat. Genet.* **38,** (suppl.), S8–S13
47. Lewis, B. P., Shih, I. H., Jones-Rhoades, M. W., Bartel, D. P., and Burge, C. B. (2003) Prediction of mammalian microRNA targets. *Cell* **115,** 787–798
48. Alexander, R. P., Fang, G., Rozowsky, J., Snyder, M., and Gerstein, M. B. (2010) Annotating non-coding regions of the genome. *Nat. Rev. Genet.* **11,** 559–571
49. Pang, K. C., Frith, M. C., and Mattick, J. S. (2006) Rapid evolution of noncoding RNAs: lack of conservation does not mean lack of function. *Trends Genet.* **22,** 1–5
50. Marques, A. C., and Ponting, C. P. (2009) Catalogues of mammalian long noncoding RNAs: modest conservation and incompleteness. *Genome Biol.* **10,** R124
51. Langmead, B., Trapnell, C., Pop, M., and Salzberg, S. L. (2009) Ultrafast and memory-efficient alignment of short DNA sequences to the human genome. *Genome Biol.* **10,** R25
52. Tabaska, J. E., and Zhang, M. Q. (1999) Detection of polyadenylation signals in human DNA sequences. *Gene* **231,** 77–86
53. Lewis, B. P., Burge, C. B., and Bartel, D. P. (2005) Conserved seed pairing, often flanked by adenosines, indicates that thousands of human genes are microRNA targets. *Cell* **120,** 15–20
54. Kong, L., Zhang, Y., Ye, Z. Q., Liu, X. Q., Zhao, S. Q., Wei, L., and Gao, G. (2007) CPC: assess the protein-coding potential of transcripts using sequence features and support vector machine. *Nucleic Acids Res.* **35,** W345–349